Biochimica et Biophysica Acta 1842 (2014) 2500–2509

Contents lists available at ScienceDirect

Biochimica et Biophysica Acta

journal homepage: www.elsevier.com/locate/bbadis

Inactivation of brain Cofilin-1 by age, Alzheimer's disease and γ-secretase

Eugenio Barone, Sebastien Mosser, Patrick C. Fraering *

Brain Mind Institute and School of Life Sciences, Ecole Polytechnique Fédérale de Lausanne (EPFL), CH1015 Lausanne, Switzerland

ARTICLE INFO

Article history:
Received 26 June 2014
Received in revised form 21 September 2014
Accepted 6 October 2014
Available online 12 October 2014

Keywords:
Alzheimer's disease
Aging
Cofilin1
γ-Secretase

ABSTRACT

Rapid remodeling of the actin cytoskeleton in the pre- and/or post-synaptic compartments is responsible for the regulation of neuronal plasticity, which is an important process for learning and memory. Cofilin1 plays an essential role in these processes and a dysregulation of its activity was associated with the cognitive decline observed during normal aging and Alzheimer's disease (AD). To understand the mechanism(s) regulating Cofilin1 activity we evaluated changes occurring with regard to Cofilin1 and its up-stream regulators Lim kinase-1 (LIMK1) and Slingshot phosphatase-1 (SSH1) in (i) human AD brain, (ii) 1-, 4-, and 10-months old APP/PS1 mice, (iii) wild type 3-, 8-, 12-, 18- and 26-months old mice, as well as in cellular models including (iv) mouse primary cortical neurons (PCNs, cultured for 5, 10, 15 and 20 days *in vitro*) and (v) mouse embryonic fibroblasts (MEF). Interestingly, we found an increased Cofilin1 phosphorylation/inactivation with age and AD pathology, both *in vivo* and *in vitro*. These changes were associated with a major inactivation of SSH1. Interestingly, inhibition of γ-secretase activity with Compound-E (10 μM) prevented Cofilin1 phosphorylation/inactivation through an increase of SSH1 activity in PCNs. Similarly, MEF cells double knock-out for γ-secretase catalytic subunits presenilin-1 and -2 (MEF_{DKO}) showed a strong decrease of both Cofilin1 and SSH1 phosphorylation, which were rescued by the overexpression of human γ-secretase. Together, these results shed new light in understanding the molecular mechanisms promoting Cofilin1 dysregulation, both during aging and AD. They further have the potential to impact the development of therapies to safely treat AD.

1. Introduction

Alzheimer's disease (AD) is the most common form of dementia among the elderly. Amyloid-β peptides (Aβ) form senile plaques, which, together with hyperphosphorylated tau-based neurofibrillary tangles (NFT), are the hallmarks of AD neuropathology [1]. From a clinical point of view, a decline in episodic memory is observed, often mistaken with normal aging-related cognitive deficiencies [1]. These similarities raised questions about the role of aging in AD onset and progression, thus demanding major efforts to clarify the molecular mechanisms underlying these processes [2].

Aβ is strongly suspected to play a major role in the development of dementia. Elevated Aβ levels produce abnormalities in learning and synaptic functions in amyloid precursor protein (APP) transgenic mice [3,4]. Furthermore, studies in human [5,6] and 3×Tg-AD mice (triple transgenic model of AD) [7] highlighted the importance of soluble endocytosed intraneuronal Aβ as the initial mediator of Tau pathology and cognitive decline. Indeed, although senile plaque-formation has been widely proposed to be responsible of the Aβ toxic effects, meticulous analyses of AD patients suggest that the soluble pool of $Aβ_{42}$ correlates better with cognitive decline than Aβ plaques [5,6,8]. Oligomers of $Aβ_{42}$ significantly (i) diminish long-term potentiation (LTP), which is needed for learning and memory [9], (ii) promote an increase of oxidative stress [10–12], (iii) impair synaptic functions [9,12]. Whether these effects are mainly due to the extracellular or to the endocytosed Aβ remain to be clarified, although disturbances in the metabolism of Aβ might regionally increase $Aβ_{42}$ levels that negatively modulate neuronal activity and potentially lead to a decline in cognitive performance [13].

Aβ peptides are derived from APP, a type I membrane protein that undergoes a first cleavage by β-secretase leading to the production of a 99 amino-acid long APP-C99 (APP-C-terminal fragment). The latter is further processed within the membrane bilayer by the intramembrane aspartyl-protease γ-secretase to generate an APP intracellular domain (AICD) released into the cytoplasm, and Aβ secreted in the extracellular compartment [14]. Despite the prominent role of γ-secretase in driving Aβ production, its involvement in the cellular pathways regulating cognitive processes is controversial because both the increase and the lack of γ-secretase activity were reported to impair synaptic function and neuronal survival [15–18]. APP is not the unique substrate for **γ**-

Abbreviations: AD, Alzheimer's disease; APP, amyloid precursor protein; APP/PS1, $APP^{KM670/671NL}$/$PS1^{L166P}$ transgenic mice; APP_{KO}, amyloid precursor protein knockout mice; Aβ, Amyloid-β peptides; Cofilin1, Cofilin isoform 1; CpdE, Compound E; DIV, days *in vitro*; DMSO, dimethyl sulfoxide; LIMK1, LIM kinase isoform 1; MEFs, mouse embryonic fibroblasts; MEF_{DKO}, MEFs lacking both catalytic subunits of γ-secretase, presenilin-1 and −2; $MEF_{DKO\ +\ hγ\text{-}secretase}$, MEF_{DKO} cell line stably overexpressing the human γ-secretase complex; NFT, neurofibrillary tangles; PCNs, primary cortical neurons; pCofilin1, phosphorylated Cofilin isoform 1; pLIMK1, phosphorylated LIM kinase isoform 1; PS1, presenilin 1; pSSH1, phosphorylated Slingshot phosphatase isoform 1; SSH1, Slingshot phosphatase isoform 1; WT, wild type

* Corresponding author.
E-mail address: patrick.fraering@epfl.ch (P.C. Fraering).

http://dx.doi.org/10.1016/j.bbadis.2014.10.004
0925-4439/

secretase, which is responsible for the cleavage of a broad range of protein receptors playing a role in neuronal trafficking and synaptic plasticity [reviewed in [19]].

Recently, modifications of γ-secretase by nitrosative stress were found to be responsible for an age-dependent increase of the $A\beta_{42}/A\beta_{40}$ ratio in rat hippocampal neurons, thus offering a new possible mechanism linking aging and AD [20]. Indeed, the accumulation of $A\beta_{42}$ would trigger a pathological mechanism leading to an aberrant neuritic morphology, sprouting and breakdown [21], which affect the structure of synapses and lead to (i) altered neuronal electrophysiology [22], (ii) inhibition of long-term potentiation [23] and (iii) transient memory deficits [24].

These phenomena strictly involve the actin cytoskeleton, which actively participates in the maturation and in the maintenance of the synapses by regulating spine morphology [25], receptor anchoring/trafficking and synaptic plasticity [26,27]. Among numerous actin-binding proteins, the actin-depolimerizing factor (ADF)/cofilin family proteins, comprising in mammals Cofilin1 (a non-muscle type), Cofilin2 (a muscle-type) and ADF (also known as destrin), critically control actin filament dynamics and reorganization by severing and depolymerizing actin filaments [28]. A growing body of evidence lends support to a link between neurite transport defects or impaired synaptic plasticity observed with age or in neurodegenerative diseases, and alterations in the organization and dynamics of the actin cytoskeleton initiated by Cofilin1 [27,29–31]. Regulation of Cofilin1 activity is quite complex and involves cross-talking pathways [30]. In particular, Cofilin1 is inactivated by LIM kinase isoform 1 (LIMK1)-mediated phosphorylation at Serine 3 (Ser3), and is reactivated by Slingshot phosphatase isoform 1 (SSH1)-mediated dephosphorylation [28]. Although other kinases and phosphatases can affect Cofilin1 activity, LIMK1 and SSH1 show the highest substrate specificity [30]. Remarkably, phosphorylation of Threonine 508 activates LIMK1 whereas phosphorylation at Serine 937 and 978 inactivates SSH1 [28]. In addition, not only Cofilin1 but also LIMK1 is a substrate for SSH1 activity, which in this way can control Cofilin1 activation either directly or indirectly through an upstream regulation of LIMK1 [32].

In this study, we show that a dysregulation of SSH1/LIMK1/Cofilin1 (hereafter, Cofilin1 pathway) occurs in the brain as an effect of both age and AD pathological features. We further demonstrate that γ-secretase activity is involved in the regulation of both Cofilin1 protein levels and phosphorylation/inactivation, providing potential new insights into the molecular mechanisms that link aging to AD.

2. Materials and methods

2.1. Human tissues

Post-mortem tissues from frontal cortex were obtained from the Joseph and Kathleen Bryan Alzheimer's Disease Research Center, Duke University Medical Center [33]. Controls were compared to patients with moderate to severe Alzheimer's disease. The age of death, gender and postmortem interval were comparable in both groups. Demographic and diagnostic features available for patients used in this study are showed in the Supplementary Table 1.

2.2. Animals

All animal procedures were performed in accordance to Swiss authority guidelines. Animals were sacrificed at the selected age, brains were extracted, weighed, flash-frozen, and stored at −80 °C until total protein extraction from one hemibrain and further analyses. Frozen brain specimens were obtained from 3-, 8-, 12-, 18- and 26-months old wild type (WT) (C57Bl/6 J) mice and 1-, 4- and 10-months old $APP^{KM670/671NL}/PS1^{L166P}$ transgenic mice (APP/PS1) mice [34] or APP knock-out (APP_{KO}) mice [35], and their littermate controls. APP/PS1 mice were studied at 1, 4 and 10 months of age, because this is the time frame during which these mice develop all pathological AD features [34]. Indeed, cerebral amyloidosis starts at 6–8 weeks, and the ratio of human amyloid Aβ42/Aβ40 is respectively 1.5 and 5 in pre-depositing (1 month-old) and amyloid-depositing mice (4 and 10 months-old). Consistent with this ratio, extensive congophilic parenchymal amyloid but minimal amyloid angiopathy is observed [34]. Amyloid-associated pathologies include dystrophic synaptic boutons, hyperphosphorylated tau-positive neuritic structures and robust gliosis, with neocortical microglia number increasing threefold from 1 to 8 months of age. Global neocortical neuron loss is not apparent up to 8 months of age, but local neuron loss in the dentate gyrus is observed. In addition, diffuse Aβ plaques are strongly increased at 8 month and defects in cognition were observed only at 8 month [34]. Because the age process in WT mice is much longer than that observed in APP/PS1 mice, we have decided not to limit the analysis of the Cofilin1 pathway in WT mice to the time points selected for APP/PS1 mice. Indeed, according to the American Federation of Aging Research criteria (http://www.afar.org/research/funding/animal-use/), 2–3 months-old mice can be considered young and they represent the biological equivalent of teen-agers and college freshmen, whereas 26 months-old mice can be considered old, taking also into consideration that a median survival is of about 24 months. Finally APP_{KO} mice [35] were studied at the same time points selected for APP/PS1 mice to test whether the changes observed in a model characterized by an accelerated APP cleavage (APP/PS1) were different in the absence of APP protein.

2.3. Cell culture and treatments

Mouse primary cortical neurons (PCNs) were prepared from embryonic day 17 Of1 mouse fetal brains. Cortices were digested in a media containing papain (20 U/ml, Sigma-Aldrich GmbH, Buchs, Switzerland) and dissociated by mechanical trituration. Cells were plated in neurobasal medium (Invitrogen, LuBioScience GmbH, Lucerne, Switzerland) supplemented with B27 (Invitrogen, LuBioScience GmbH, Lucerne, Switzerland) and 2 mM L-glutamine on poly-L-ornythine coated plates at 1×10^5 cells/cm^2 at 37 °C in a humidified 5% CO2 atmosphere. At day 5, 10, 15 and 20, neurons were washed twice with PBS and proteins were extracted as described below. The criteria to univocally establish at what age *in vitro* PCNs reflect aging neurons *in vivo* do not appear very clear due to divergent interpretations. Indeed, from one side, it was reported that during the first week, *in vitro* mouse PCNs establish morphological and functional axons and dendrites; during the second week they establish synaptic activity and from the third week on (14 DIV) they begin to show canonical signs of aging, including (i) accumulation of ROS, (ii) lipofuscin granules, (iii) heterochromatic foci, (iv) activation of the c-Jun N-terminal protein kinase (JNK) and (v) the DNA repair p53/p21 pathways as well as (vii) cholesterol loss and (viii) increased cholesterol-24-hydroxylase [36–38]. In addition, *in vitro* hippocampal neurons cultured for 3 weeks (21 DIV) undergo a time-associated increase in tubulin acetylation similar to that observed *in vivo*, and a time-associated increase in the phosphorylation of the microtubule-associated protein Tau [38] similar to those reported either in aged human brains [39] or in mouse models of senescence [40]. On the other side, it has been shown that starting at 28 DIV, mouse PCNs present a time-dependent and significant increase in known features of the aging brain, including protein oxidation, creatine kinase expression and calcium channel density [41,42]. In addition, based on phase contrast microscopy and the evaluation of the neuronal nuclear protein NeuN levels in mouse PCNs cultured from 5 to 60 DIV, it seems that (i) 20–25 DIV cultured neurons show typical signs of neuronal maturation, while (ii) only a subset of the neuronal population survives through DIV60 [43]. Thus, this spontaneous age-related loss of neurons supports an important distinction between DIV 20–25 neurons ("matured neurons") and DIV60 neurons ("aged neurons"). Based on the above-cited information, 20 DIV neurons used in this study may better reflect mature-to-old neurons *in vivo*, and not exclusively aging neurons in the brain. To test γ-secretase activity-dependent changes of

Cofilin1 pathway, the day before the selected time points, neurons were treated overnight with DMSO (0.25%) or γ-secretase inhibitor Compound E (CpdE) (10 μM, Merck Millipore, Darmstadt, Germany) and then subjected to Western Blot analysis as described below. Mouse Embryonic Fibroblasts: (i) wild-type (MEF), (ii) double knock-out for presenilin-1 (PS1) and -2 (PS2) [MEF_{DKO}, [44,45]] and (iii) double knock-out overexpressing the human γ-secretase complex [$MEF_{DKO\ +\ h\gamma\text{-secretase}}$, [46]] were grown in 10 cm dishes in DMEM, supplemented with 10% fetal bovine serum (FBS) and penicillin/streptomycin (P/S) (Invitrogen, LuBioScience GmbH, Lucerne, Switzerland).

2.4. Western Blot

Total protein extracts were prepared in 1% NP40–HEPES buffer (50 mM HEPES, pH 7.0, 150 mM NaCl, 5 mM MgCl2, 5 mM CaCl2), supplemented with protease inhibitor cocktail (Roche, Rotkreuz, Switzerland), and were clarified by centrifugation for 1 h at 16,000 ×*g*, 4 °C. Protein concentrations were determined using standard BCA assay (Pierce, Rockford, IL, USA). Ten micrograms of protein were resolved on 4–12% Bis-Tris PAGE gels (Invitrogen, LuBioScience GmbH, Lucerne, Switzerland), or on standard 12% acrylamide/bisacrylamide Tris Glycine gels for SDS-PAGE analysis. For immunoblot analysis, gels were transferred onto nitrocellulose membranes (Whatman, Dassel, Germany), and incubated overnight at 4 °C with the following antibodies: anti-Cofilin1 612144 (1:1000, Bd Transduction Laboratories, Allschwil, Switzerland) anti-phospho(Ser3)-Cofilin1 3311 s (1:500, Cell Signaling, Bioconcept, Allschwill, Switzerland), anti-phospho(Ser3)-Cofilin1 ab12866 (1:1000, abcam, Cambridge, United Kingdom), anti-LIMK1 ab87971 (1:1000, abcam, Cambridge, United Kingdom), anti-phospho(Thr508)-LIMK1 ab38508 (1:500, abcam, Cambridge, United Kingdom), anti-SSH1 ab107799 (1:1000, abcam, Cambridge, United Kingdom), anti-phospho(Ser978)-SSH1 SP3901 (1:500, ECM Biosciences, Versailles, KY, USA), anti-PS1 ab10281 (1:1000, abcam, Cambridge, United Kingdom), anti-APP-C terminal fragments (CTFs) A87717 (1:10,000, Sigma-Aldrich, GmbH, Buchs, Switzerland), anti-Chronophin 4686 (1:500, Cell Signaling, Bioconcept, Allschwill, Switzerland) and anti-β-actin A2066 (1:5000, Sigma-Aldrich GmbH, Buchs, Switzerland). Membranes were developed by using anti-mouse/rabbit/rat IgG conjugated to Alexa 680 or 800 purchased from Invitrogen (LuBioScience GmbH, Lucerne, Switzerland). The Odyssey infrared imaging system (LICOR, Bad Homburg, Germany) was used to detect the fluorescent signal. For each antibody used in this study, a dose–response analysis was performed by loading 15–40 μg total proteins from 3 months-old WT mouse brain whole homogenate — this is to correlate changes observed in signal strength with changes observed at the protein levels (Supplementary Fig. 1). As shown in Supplementary Fig. 1, all signals exhibit linearity at the protein levels tested and the protein amount (30 μg) we used for sample analysis all over the manuscript falls into this linear range.

2.5. Aβ quantification

Cultures media from 5, 10, 15 and 20 days *in vitro* (DIV) neurons were collected, protease inhibitor cocktail (Roche, Rotkreuz, Switzerland) added, and Aβ peptides were quantified using mouse $Aβ_{40}$ and $Aβ_{42}$ ELISA kits (KHB3481, KHB3441; Invitrogen, LuBioScience GmbH, Lucerne, Switzerland).

2.6. Statistical analysis

All experiments were performed at least twice with comparable results, and all data are presented as means ± SEM of n independent samples per group. Student's *t* test was applied for statistical analysis. $P < 0.05$ was considered significantly different from the reference value.

3. Results

3.1. The Cofilin1 activation state is altered in AD human brains

Hyperactive cofilin forming rod-shaped cofilin-saturated actin filament bundles (rods) were previously reported over Aβ plaques in the hippocampus of AD subjects, suggesting abnormal Cofilin1 aggregation in response to neurodegenerative stimuli [47,48]. Because of the pivotal role of γ-secretase in driving AD pathology and based on a significant increase of its activity in the brain of sporadic AD subjects [49], we analyzed the Cofilin1 pathway in the frontal cortex of seven sporadic AD subjects (average age 87.8 ± 1.6 years) and their age-matched controls (average age 82.6 ± 2.7 years) [33]. As shown in Fig. 1, a significant ~1.6 fold-increase of the pCofilin1/Cofilin1 ratio (Fig. 1-c) is observed in the frontal cortex of AD subjects with respect to controls, suggesting that Cofilin1 gets inactivated in diseased brains. To extend our knowledge about the mechanisms responsible for Cofilin1 inactivation in AD, we further demonstrated defects in SSH1 activity. As shown in Fig. 1-g, a ~45% significant reduction of total SSH1 protein levels associated with

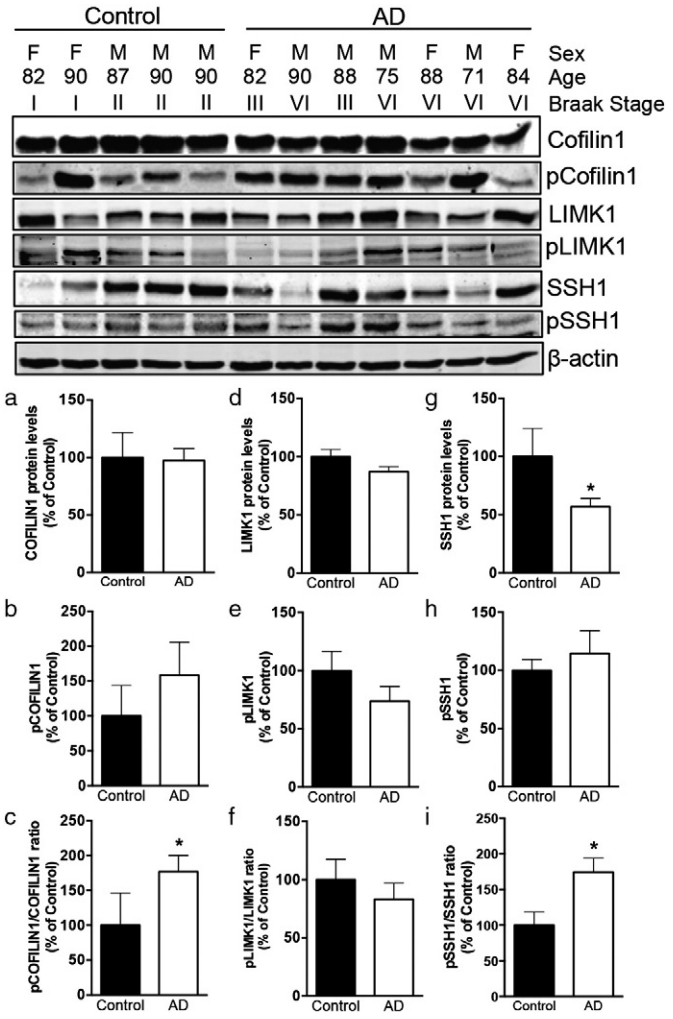

Fig. 1. Cofilin1 inactivation in the frontal cortex of sporadic human Alzheimer's disease. Changes observed with regard to the Cofilin1 pathway in the frontal cortex of sporadic Alzheimer's disease subjects (n = 7), relative to their age-matched controls (n = 5). *Top panels*: Western blot analyses of total protein extracts. *Bottom panels*: densitometric analyses of Western blot protein bands: (a) Total Cofilin1 protein levels; (b) pCofilin1 levels; (c) pCofilin1/Cofilin1 ratio; (d) Total LIMK1 protein levels; (e) pLIMK1 levels; (f) pLIMK1/LIMK1 ratio; (g) Total SSH1 protein levels; (h) pSSH1 levels; (i) pSSH1/SSH1 ratio. Protein levels were normalized to the loading control β-actin. Densitometric values shown in the histograms are given as percentage of Control samples set as 100%. Means ± SEM, *P < 0.05 *vs* Control.

unchanged pSSH1 levels led to the significant increase of the pSSH1/SSH1 ratio (Fig. 1-i). The latter suggests an inactivation of SSH1 in AD brains. No significant changes were observed for LIMK1 protein levels and phosphorylation (Fig. 1-d–f). Altogether, these observations suggest that the increased Cofilin1 inactivation observed in our AD samples could be mediated, at least in part by the loss of SSH1 activity.

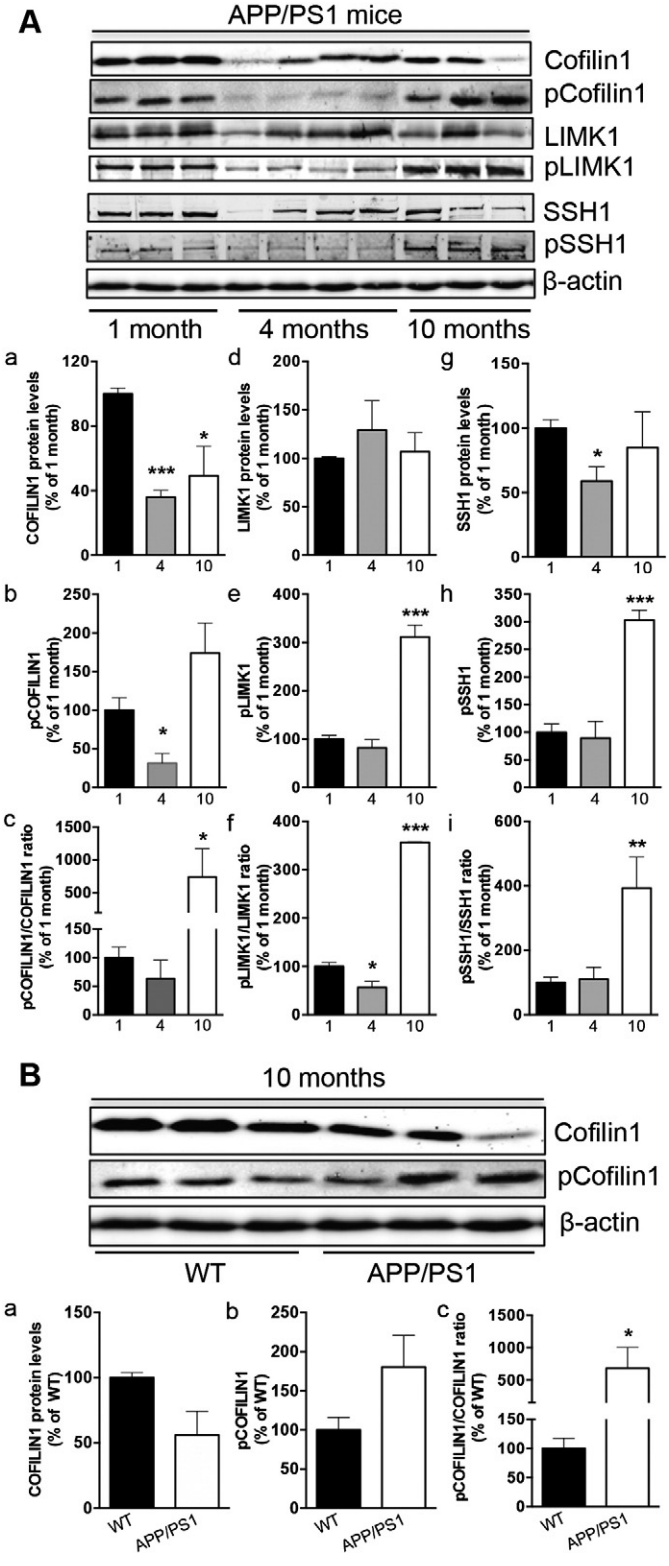

3.2. AD pathology-associated inactivation of Cofilin1 in the brain of APP/PS1 mice

To better understand the altered pattern of expression/activation of Cofilin1 in AD, we analyzed changes of the Cofilin1 pathway in 1-, 4-, and 10-months old APP/PS1 mice [34], a well-known model of AD characterized by age-associated increase of pathological features including Aβ senile plaques and cognitive deficits [34]. As shown in Fig. 2A-a, Cofilin1 protein levels are significantly reduced by ~65% and ~50% at 4- and 10-months of age, with respect to 1 month-old mice. The analysis of pCofilin1 further revealed a significant ~70% decrease at 4 months of age, whereas an increase of about 70% was observed at 10 months (Fig. 2A-b). Interestingly, 10-months old APP/PS1 mice showed a 7-fold increase in the pCofilin1/Cofilin1 ratio, with respect to the young, 1-month old mice (Fig. 2A-c). In order to assess whether alteration of Cofilin1 phosphorylation can be explained by modifications of its upstream regulators, we next evaluated changes occurring for LIMK1 and SSH1. As shown in Fig. 2A-d, total LIMK1 did not show any significant changes at 1-, 4- and 10-months. Conversely, pLIMK1 levels were drastically increased (by ~ 200%) at 10-months of age, with respect to the 1 month-old mice (Fig. 2A-e). Consequently, the pLIMK1/LIMK1 ratio showed a 3.5-fold increase at 10-months (Fig. 2A-f), suggesting an overactivation of LIMK1 in aged mice. With regard to SSH1 phosphatase the most drastic effect was observed for the inactive pSSH1 at 10-months of age, with an increase of ~ 200% with respect to 1 month-old mice (Fig. 2A-h). As a consequence, a 3.9-fold increase of the pSSH1/SSH1 ratio was observed (Fig. 2A-i), suggesting an inactivation of SSH1 in aged mice.

Finally, in order to evaluate whether the increased phosphorylation/inactivation of Cofilin1 in 10 months-old APP/PS1 mice was the result of AD-related pathology, the Cofilin pathway was examined in APP/PS1 mice and their littermate WT controls. As shown in Fig. 2B, Cofilin1 and pCofilin1 protein levels were respectively reduced by ~ 45% (Fig. 2B-a) and increased by ~80% (Fig. 2B-b) in AD mice, with respect to the littermate matched WT controls. As a consequence of these changes, the pCofilin1/Cofilin1 ratio showed a significant 6-fold increase (Fig. 2B-c), suggesting again an inactivation of Cofilin1 in AD mice. These lines of evidence parallel with changes observed with regard to LIMK1 and SSH1. Indeed, in APP/PS1 mice both LIMK1 and SSH1 protein levels were reduced by ~40% (Supplementary Fig. 2-a and b), while pLIMK1 and pSSH1 levels were significantly increased by ~40% and ~140%, respectively (Supplementary Fig. 2-b and e). The drastic increases of both pLIM1/LIMK1 (~2.5-fold, Supplementary Fig. 2-c) and pSSH1/SSH1 (~5-fold, Supplementary Fig. 2-f) ratios suggest again an activation of LIMK1 and an inactivation of SSH1 in the brain of 10-months old AD mice.

3.3. Age-dependent Cofilin1 inactivation in the brain of WT mice

We next investigated whether aging, in the absence of AD, plays a role in the Cofilin pathway alterations observed in AD human/mice

Fig. 2. Alzheimer's disease pathology-associated changes of the Cofilin1 pathway proteins in the brain of APP/PS1 mice. (A) Age-dependent changes observed with regard to proteins controlling the Cofilin1 pathway, in the brain of 1- (n = 3), 4- (n = 4) and 10-months old (n = 3) APP/PS1 mice. Top panels: Western blot analyses of total protein extracts. Bottom panels: densitometric analyses of Western blot protein bands: (a) Total Cofilin1 protein levels; (b) pCofilin1 levels; (c) pCofilin1/Cofilin1 ratio; (d) Total LIMK1 protein levels; (e) pLIMK1 levels; (f) pLIMK1/LIMK1 ratio; (g) Total SSH1 protein levels; (h) pSSH1 levels; (i) pSSH1/SSH1 ratio. (B) Decreased total Cofilin1 protein levels and increased pCofilin1 levels in 10-months old APP/PS1 mice (n = 3), with respect to their littermate WT controls (n = 3). *Top panels*: Western blot analyses of total protein extracts. *Bottom panels*: densitometric analyses of Western blot protein bands: (a) Total Cofilin1 protein levels; (b) pCofilin1 levels; (c) pCofilin1/Cofilin1 ratio. Protein levels were normalized to the loading control β-actin. Densitometric values shown in the histograms are given as percentage of 1 month-old mice (A) or WT mice (B) set as 100%. Means ± SEM, *P < 0.05, **P < 0.01 and ***P < 0.001 *vs* Control (A) or WT (B).

samples. To do so, we evaluated changes in the Cofilin pathway occurring in the brains of 3-, 8-, 12-, 18- and 26-month old WT mice. When compared to 3-month old mice, Cofilin1 protein levels were significantly reduced by ~25% both at 8 and 26 months (Fig. 3-a). Yet, the major change was observed for pCofilin1, which was increased by ~76% in the oldest 26 months-old mice (Fig. 3-b), leading to a ~2.3-fold increase of the pCofilin1/Cofilin1 ratio (Fig. 3-c). No significant differences were observed for LIMK1 total and phosphorylated protein levels (Fig. 3-d–e). In contrast, an interesting trend was observed for pSSH1. After a significant reduction at both 8 and 12 months (by ~45% and ~35%, respectively), pSSH1 levels significantly raised (by ~27%) at 26 months (Fig. 3-h). Together, and despite the drastic increase of both pCofilin1 levels and pCofilin1/Cofilin1 ratio, no significant changes were found for both pLIMK1/LIMK1 and pSSH1/SSH1 ratios in 26 months-old mice (Fig. 3-f and i). At a first glance, the latter observation does not explain changes observed with regard to Cofilin1. However, an in-depth analysis of the results suggests that 8 months possibly represents a turning point in the aging process occurring in our mice. Indeed, from 8 to 26 months, a clear increase of pCofilin1 occurs (Fig. 3-b), possibly caused by an age-dependent inactivation of SSH1 revealed by the rise of the pSSH1 levels (Fig. 3-h) and the pSSH1/SSH1 ratio (Fig. 3-i) in the same time frame.

3.4. Inactivation of Cofilin1 during neuronal maturation in vitro

We next assessed whether changes in the Cofilin1 pathway could be observed during neuronal maturation, in mouse PCNs cultured for 5, 10, 15 and 20 days. These time points were selected because (i) an increase of synaptic density [50], (ii) a linear increase of Aβ production [51] and (iii) a shift with regard to γ-secretase activity towards more amyloidogenic pathways [20] occur within this time frame. Also, primary neuronal cultures undergo a whole series of morphological and functional maturation processes that reflect at least partially those of their counterparts *in vivo* [20,36,37,41,42,52]. As shown in Fig. 4-a and b, Cofilin1 and pCofilin1 protein levels were respectively reduced and increased in an age-dependent manner from 5 to 20 DIV (Fig. 4-a). These changes led to age-dependent increases in the pCofilin1/Cofilin1 ratio, starting at 10 DIV (~2.6 fold), increasing at 15 DIV (~3.3 fold) and reaching the maximum at 20 DIV (~4.5 fold), with respect to 5 DIV (Fig. 4-c). Similarly, changes of total LIMK1 (Fig. 4-d) and pLIMK1 (Fig. 4-e) protein levels lead to an age-dependent increase in the pLIMK1/LIMK1 ratio, reaching about 75% at 20 DIV (Fig. 4-f). Interestingly, significant and age-associated increases in SSH1 and pSSH1 protein levels were also observed (Fig. 4-g and h), causing a marked increase in the pSSH1/SSH1 ratio both at 15 DIV (~1.9-fold)

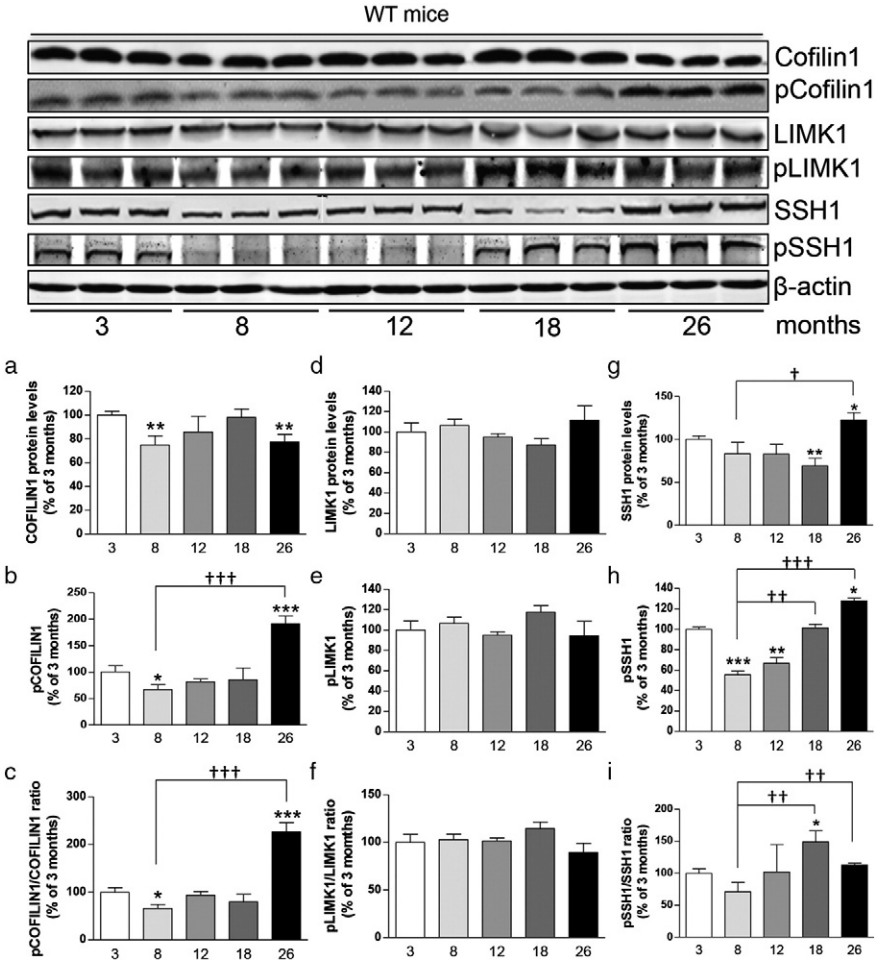

Fig. 3. Age-associated changes of the Cofilin1 pathway in the brain of WT mice. Age-associated changes observed with regard to proteins implicated in the Cofilin1 pathway, in the brain of 3- (n = 5), 8- (n = 4), 12- (n = 5), 18- (n = 5) and 26-months old (n = 4) WT mice. Representative gels obtained with 3 blind selected samples per group are shown. *Top panels*: Western blot analyses of total protein extracts. *Bottom panels*: densitometric analyses of Western blot protein bands: (a) Total Cofilin1 protein levels; (b) pCofilin1 levels; (c) pCofilin1/Cofilin1 ratio; (d) Total LIMK1 protein levels; (e) pLIMK1 levels; (f) pLIMK1/LIMK1 ratio; (g) Total SSH1 protein levels; (h) pSSH1 levels; (i) pSSH1/SSH1 ratio. Protein levels were normalized to the loading control β-actin. Densitometric values shown in the histograms are given as percentage of 3 months-old mice set as 100%. Means ± SEM, *P < 0.05, **P < 0.01 and ***P < 0.001 *vs* 3-months old mice; †P < 0.05, ††P < 0.01 and †††P < 0.001 *vs* 8-months old mice.

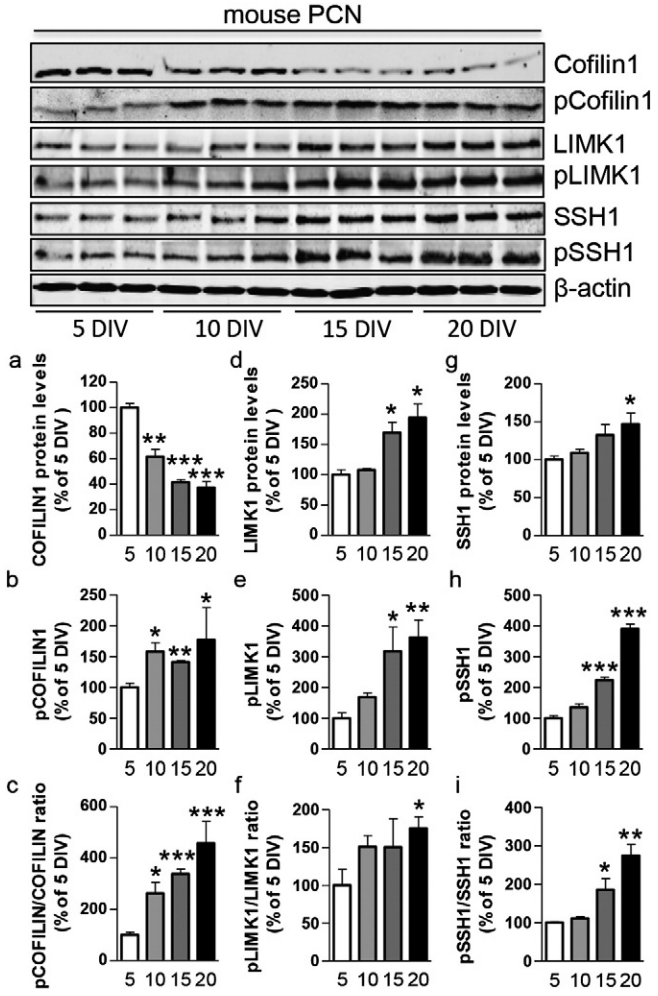

Fig. 4. Cofilin1 pathway changes during mouse primary cortical neurons (PCNs) maturation *in vitro*. Age-associated changes of proteins from the Cofilin1 pathway in mouse PCNs at 5, 10, 15, and 20 days *in vitro* (DIV) (n = 3 independent cultures/group). *Top panels*: Western blot analyses of total protein extracts. *Bottom panels*: densitometric analyses of Western blot protein bands: (a) Total Cofilin1 protein levels; (b) pCofilin1 levels; (c) pCofilin1/Cofilin1 ratio; (d) Total LIMK1 protein levels; (e) pLIMK1 levels; (f) pLIMK1/LIMK1 ratio; (g) Total SSH1 protein levels; (h) pSSH1 levels; (i) pSSH1/SSH1 ratio. Protein levels were normalized to the loading control β-actin. Densitometric values shown in the histograms are given as percentage of 5 DIV PCNs set as 100%. Means ± SEM, $^{*}P < 0.05$, $^{**}P < 0.01$ and $^{***}P < 0.001$ *vs* 5 DIV.

and at 20 DIV (~2.7-fold), in comparison to the younger 5 DIV neurons (Fig. 4-i). Altogether, both LIMK1 activation (Fig. 4-f) and SSH1 inactivation (Fig. 4-i) with age are very consistent with the observed Cofilin1 inactivation (Fig. 4-c).

3.5. γ-Secretase is a negative regulator of Cofilin1 activation

In agreement with previous results [20], we observed in our PCNs cultures that increased secreted $A\beta_{42}$ and $A\beta_{40}$ levels (Supplementary Fig. 3A) are associated with changes of the $A\beta_{42}/A\beta_{40}$ ratio, from 5 to 20 DIV (Supplementary Fig. 3B). These changes include a switch towards the production of the more amyloidogenic $A\beta_{42}$ peptides, possibly suggesting age-dependent modifications of the γ-secretase specific activity. Because of that observation, we further hypothesized that γ-secretase activity can affect the Cofilin1 pathway, possibly in an age-dependent manner. To challenge this hypothesis, 5, 10, 15 and 20 DIV mouse PCNs were treated for 24 h with 10 μM of CpdE, a potent γ-secretase inhibitor. First, we found that DMSO alone did not affect Cofilin-1 protein levels and phosphorylation changes observed in untreated neurons with age (Fig. 5A-a–c). Conversely, inhibition of γ-secretase activity promotes a significant decrease (by about 35%) of total Cofilin1 levels, only at 20 DIV with respect to DMSO-treated PCNs (Fig. 5A-a). Importantly, pCofilin1 levels were reduced at 10, 15 and 20 DIV (by ~40%, ~50% and ~50, respectively) in CpdE-treated neurons, reaching statistical significance at 15 DIV and 20 DIV (Fig. 5A-b). Together, a significant decrease of the pCofilin1/Cofilin1 ratio was observed in CpdE-treated neurons at 10 DIV (~1.5 fold), 15 DIV (~1.4 fold) and 20 DIV (~1.3 fold) (Fig. 5A-c). Since we observed a γ-secretase dependent reduction of both total Cofilin1 and pCofilin1 protein levels only in 20 DIV neurons, and since older PCNs showed a significant increase in the $A\beta_{42}/A\beta_{40}$ ratio (Supplementary Fig. 3B), we decided to further evaluate the effect of γ-secretase activity on LIMK1 and SSH1 in 20 DIV PCNs. As shown in Figs. 5B-d,e, inhibition of γ-secretase did not affect LIMK1 protein levels or phosphorylation. Conversely, we observed a drastic ~50% decrease of pSSH1 levels in CpdE-treated neurons, with respect to DMSO-treated cells (Fig. 5B-h). The consistent reduction of pSSH1 levels together with no changes of SSH1 levels resulted in a strong ~1.6-fold reduction of the pSSH1/SSH1 ratio (Fig. 5B-i). Altogether, these results suggest that γ-secretase activity could induce Cofilin1 phosphorylation through the inhibition of SSH1. To exclude any off-target phenotype caused by the use of a chemical γ-secretase inhibitor, we next analyzed the Cofilin pathway in MEF_{DKO} cells characterized by a complete genetic inhibition of γ-secretase activity, caused by the knock-out of both PS1 and PS2 catalytic subunits [44,45]. In this cell line, and with respect to MEFs WT, we found decreased total Cofilin1 (~50%, Fig. 5C-a) and pCofilin-1 (~70%, Fig. 5C-b) levels, as well as a reduced pCofilin1/Cofilin1 ratio (~1.4-fold, Fig. 5C-c). A significant decrease was also observed for SSH1 protein levels (~30%, Fig. 5C-d) and phosphorylation (~45%, Fig. 5C-e), as well as for pLIMK1 (~35%, Supplementary Fig. 4B-b). To confirm that changes observed in MEF_{DKO} cells were indeed dependent on γ-secretase activity, we took advantage of the $MEF_{DKO\ +\ h\gamma\text{-secretase}}$ stable cell line previously generated in our laboratory [46], and that is characterized by a rescued γ-secretase activity via the overexpression of human γ-secretase. When compared to MEF_{DKO} cells, restored γ-secretase activity triggers a significant increase of pCofilin1 (~80%, Fig. 5C-b), to levels comparable to those of the control MEFs WT cell line. Furthermore, both SSH1 total protein levels and phosphorylation were rescued in $MEF_{DKO\ +\ h\gamma\text{-secretase}}$ (Fig. 5C-d and C-e) and a net increase of the pSSH1/SSH1 ratio with respect to MEF_{DKO} cells was observed (Fig. 5C-f). These results are in good agreement with those obtained in mouse PCNs treated with CpdE and suggest a role for γ-secretase in SSH1-mediated regulation of Cofilin1 phosphorylation/inactivation.

4. Discussion

The mechanisms by which Cofilin1 regulates cognitive processes remain quite controversial, as either an excessive activation [47,48,53–56] or inactivation [27,31,57–61] have been reported to contribute to the actin-dependent impairment of synaptic plasticity, and thus learning.

Here we provide new data about changes in the Cofilin1 pathway with age and AD. The significant increase of the pCofilin1/Cofilin1 ratio (Figs. 1, 2A-c and B-c) suggest that Cofilin1 gets inactivated in the brain of AD patients and APP/PS1 mice as a consequence of AD pathology. Furthermore, the age-associated changes observed in WT mice (Fig. 3) and mouse PCNs (Fig. 4), indicate that Cofilin1 inactivation could also be an age-dependent event. To unravel if Cofilin1 inactivation is a cause or a consequence of AD pathology needs further investigation. So far, based on our data, the significant increase of pCofilin1/Cofilin1 ratio in the brain of 10-months old APP/PS1 mice compared to the littermate WT controls (Fig. 2B-c), suggests that AD pathology could accelerate the aging process via Cofilin1 phosphorylation.

Yet, Kim et al. recently reported a decrease of the pCofilin1/Cofilin1 ratio in the frontal cortex of sporadic AD patients [56]. Interestingly, and possibly explaining this apparent discrepancy, an in-depth analysis of the latter study revealed a major difference with regard to our work, concerning the age of the subjects analyzed. Indeed, brain samples analyzed in the Kim study came from younger patients (average age; Controls: 59.6 ± 4.4; AD: 62.5 ± 0.6), when compared to the cortical samples characterized in our study, and collected from older patients (Controls: 87.8 ± 1.6 years; AD: 82.6 ± 2.7 years). Because the same antibodies were used in both studies for the analysis by Western blot of Cofilin1 levels, the apparent discrepancy cannot be attributed to the use of different technical approaches (Supplementary Fig. 5), thus

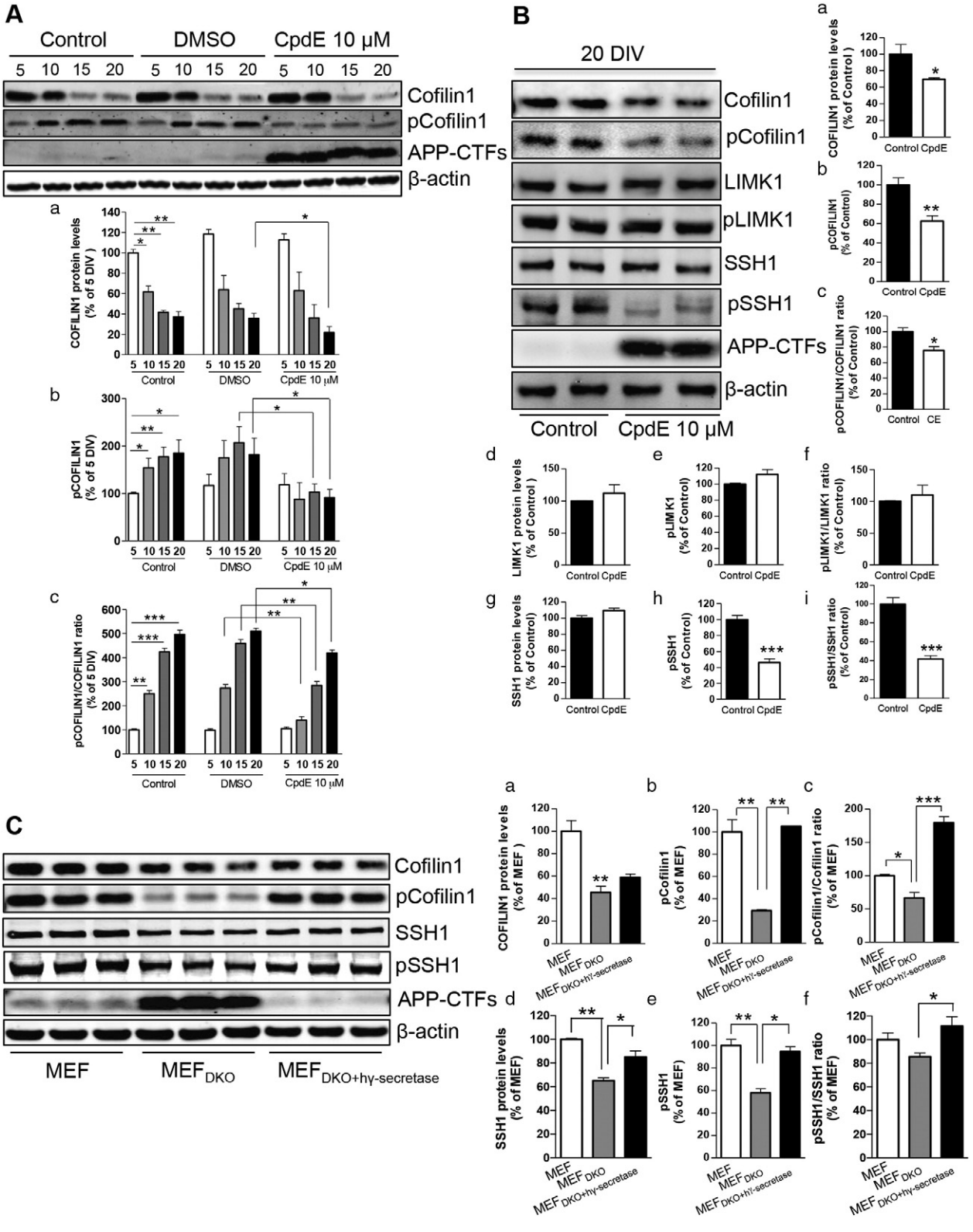

reinforcing our findings supporting a role of both age and AD pathology in the Cofilin1 pathway regulation.

Interestingly, increased pCofilin1 was also observed in maturing mouse PCNs (Fig. 4-b,c), consistent (i) with the role of Cofilin1 in dendritic spine maturation [25,27,28,62] and (ii) the observed increase of synapses density from 5 to 21 DIV [50,63]. Because either loss or inactivation of Cofilin1 is associated with spine morphology alteration and impaired associative learning and extinction memory [27,29,59,63,64] as well as inhibition of long-term depression (LTD) of the N-methyl-D-aspartate (NMDA) receptors [58], it is conceivable that an aberrant inactivation of Cofilin1 observed in human AD brain and both aged WT and APP/PS1 mice (Figs. 1–3) could be responsible for the negative effects on synaptic plasticity and cognition [27,29,59,60,64–67]. This would represent an intriguing link between age and AD pathology (Fig. 6).

The mechanisms driving Cofilin1 activation or phosphorylation/inactivation may be different and dependent, at least in part, on Aβ levels and aggregation state [53–57]. Most importantly, soluble and fibrillary Aβ may differentially affect Cofilin1 by promoting either its activation [53] or its inactivation [57]. Whether these events could happen simultaneously or sequentially still remains unclear. Based on our results in APP/PS1 mice, it seems that — with the progression of AD pathology an activation of Cofilin1 occurs at 4 months of age (Fig. 2A-b and Supplementary Fig. 6B-b) followed by a strong inactivation at 10 months (Fig. 2A-b,c and B-c), probably associated with the different pattern of Aβ deposition in the brain of these mice [34]. From a molecular point of view, Aβ peptides can differentially impact LIMK1 [30,68] whose activity was found dysregulated in AD and other neurodegenerative disorders [57,69,70]. The novelty of our work is to show for the first time the inactivation of SSH1 in AD brain (Figs. 1-i, 2A-h,i and B-c), thus strengthening the hypothesis that the equilibrium between LIMK1 and SSH1 activities is disrupted in AD. Within that frame, the significant correlations found between pCofilin1 or pCofilin1/Cofilin1 ratio and (i) SSH1 inactivation or (ii) LIMK1 activation in APP/PS1 (Supplementary Fig. 7A-a–g) and WT mice (Supplementary Fig. 8-a–d), as well as in mouse PCNs (Supplementary Figs. 9-a–c and 4A-a–d) likely account for a main role of these two upstream effectors in mediating Cofilin1 dysregulation.

To better understand the molecular mechanisms underlying the observed increase of Cofilin1 phosphorylation both *in vivo* and *in vitro*, we assessed the involvement of γ-secretase (one of the main proteins responsible of Aβ production) in these processes. A striking finding was that both chemical and genetic inhibition of γ-secretase activity promoted a significant decrease of pCofilin1 and pCofilin1/Cofilin1 ratio, and that this effect was associated with a reduction of SSH1 inhibition (Fig. 5A, B and C). This finding was further supported by the observation that overexpression of human γ-secretase in MEF_{DKO} rescued the observed phenotype (Fig. 5C-b,c and C-e,f), suggesting that γ-secretase activity might promote Cofilin1 phosphorylation through SSH1 inactivation. These changes could result from the reduced processing of one or more γ-secretase substrates whose cleavage products, in turn, regulate cell fate decision [19]. In this regard, APP represents a good candidate substrate. Indeed, the significant decrease of both pCofilin1 and relative pCofilin1/Cofilin1 ratio observed in APP_{KO} mice versus WT mice (Supplementary Fig. 10A-a and B-a) resemble the results obtained following chemical inhibition of γ-secretase activity in mouse PCNs (Fig. 5A and B), or genetic inhibition γ-secretase in MEF_{DKO} cells (Fig. 5C). Similarly, the increase of both Cofilin1 and SSH1 phosphorylation/inactivation following APP overexpression in MEF cells (Supplementary Fig. 11) recall what we observed in AD brain (Figs. 1 and 2). To unravel whether these changes are directly linked to the loss (APP_{KO} mice) or to an increase (MEF overexpressing APP) of the γ-secretase-dependent cleavage of APP needs further investigations, especially because no significant changes were observed with regard to LIMK1 (Supplementary Fig. 10A-b and B-b), SSH1 (Supplementary Fig. 10A-c and B-c) or Chronophin phosphatase (Supplementary Fig. 10A-d and B-d) in APP_{KO} mice.

Finally, early-onset familial Alzheimer's disease (FAD)-linked PS1 mutants have been reported to cause a drastic loss of γ-secretase activity in cell-free [46], cell-based [71] and *in vivo* [15] experiments. As previously observed *in vivo* [72,73], this loss-of-function is asymmetrical as all FAD-linked PS1 mutants seem to generate higher $Aβ_{42}/Aβ_{40}$ ratio compared to PS1-WT. It consequently causes an increased production of the longer and more hydrophobic Aβ species, namely Aβ, that accumulates and aggregates early in the course of the disease. Thus, one could anticipate that FAD-linked PS1 mutants would promote Cofilin1 phosphorylation, in line with (i) the observation that fibrillary Aβ promotes Cofilin1 phosphorylation [57], and (ii) our preliminary results showing that PS1-L166P promotes Cofilin1 phosphorylation (see Supplementary Fig. 12).

5. Conclusions

In conclusion, our work demonstrates an age-dependent increase of Cofilin1 phosphorylation, both in maturating PCNs and in WT mice, which resembles the Cofilin1 phenotype observed in sporadic human AD brain. γ-Secretase seems to play a fundamental role in the proposed mechanism by enhancing Cofilin1 phosphorylation via SSH1 inhibition (Fig. 6). The implication of these results on understanding the molecular mechanisms leading to impaired synaptic plasticity both during aging and AD are profound, and offer a molecular bridge connecting age, AD and the activity of γ-secretase. They further have the possibility to impact the development of therapies to treat AD.

Disclosure statement

The authors all state that there are no conflicts of interests associated with the research presented in this paper.

Acknowledgements

The authors thank M. Staufenbiel for the APP_{KO} mice (a kind gift from Novartis, Basel, Switzerland), M. Jucker for the APP/PS1 mice, B. De Strooper for the MEF_{DKO} cell line, and the Kathleen Bryan Alzheimer's Disease Research Center, Duke University Medical Center funded by NIA grant P30AG028377 for Alzheimer's disease brain tissue samples [33]. The funders had no role in study design, data collection and analysis, decision to publish, or preparation of the manuscript. This work was supported by the Swiss National Science Foundation (to P.C.F., grant 31003A_134938/1), and the Strauss foundation (to P.C.F. and E.B.).

Fig. 5. Chemical and genetic inhibition of γ-secretase activity is associated with Cofilin1 activation. (A) Inhibition of γ-secretase activity with 10 μM Compound E (CpdE) promotes Cofilin1 activation in mouse PCN at 10, 15 and 20 DIV (n = 3 independent cultures/group). A representative WB is shown. *Top panels*: Western blot analyses of total protein extracts. *Bottom panels*: densitometric analyses of Western blot protein bands: (a) Total Cofilin1 protein levels; (b) pCofilin1 levels; (c) pCofilin1/Cofilin1 ratio. (B) Cofilin1 protein levels and phosphorylation are decreased following γ-secretase activity inhibition with 10 μM Compound E (CpdE) in mouse PCN at 20 DIV (n = 4 independent cultures/group). Activation of Cofilin1 parallels with a decrease of SSH1 phosphorylation. A representative WB is shown. *Top left panels*: Western blot analyses of total protein extracts. *Bottom and right panels*: densitometric analyses of Western blot protein bands: (a) Total Cofilin1 protein levels; (b) pCofilin1 levels; (c) pCofilin1/Cofilin1 ratio; (d) Total LIMK1 protein levels; (e) pLIMK1 levels; (f) pLIMK1/LIMK1 ratio; (g) Total SSH1 protein levels; (h) pSSH1 levels; (i) pSSH1/SSH1 ratio. (C) Cofilin1 protein levels and phosphorylation are decreased in mouse embryonic fibroblast (MEF) cells lacking presenilin-1 and -2, the catalytic subunits of the γ-secretase complex (MEF_{DKO}). These changes parallel with a decrease of SSH1 protein levels and phosphorylation. Overexpression of the human γ-secretase complex in MEF_{DKO} cells ($MEF_{DKO\ +\ hγ\text{-}secretase}$) rescues Cofilin1 phosphorylation (pCofilin1) through the increase of SSH1 inactivation (pSSH1) (n = 3 independent cultures/group). *Left panels*: Western blot analyses of total protein extracts. *Right panels*: densitometric analyses of Western blot protein bands: (a) Total Cofilin1 protein levels; (b) pCofilin1 levels; (c) pCofilin1/Cofilin1 ratio; (d) Total SSH1 protein levels; (e) pSSH1 levels; (f) pSSH1/SSH1 ratio. Protein levels were normalized to the loading control β-actin. Densitometric values shown in the histograms are given as percentage of 5 DIV PCNs (Aa–Ac), untreated Control PCNs (Ba–Bi) and uninfected WT MEF (Ca–Cf) set as 100%. Means ± SEM, *P < 0.05, **P < 0.01 and ***P < 0.001.

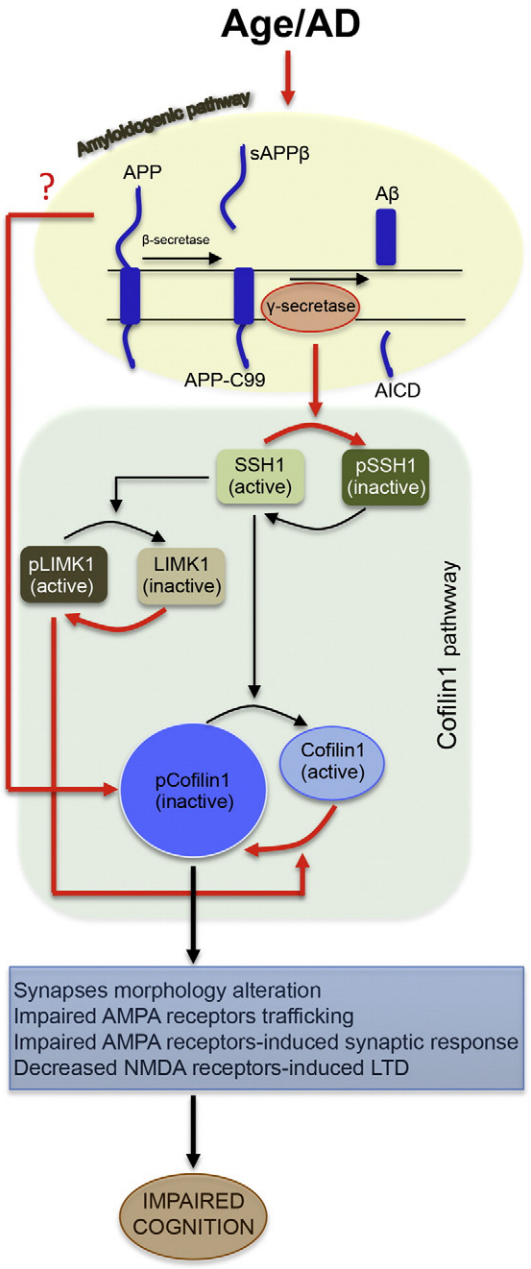

Fig. 6. Model for Age, Alzheimer's disease and γ-secretase-dependent Cofilin1 inactivation. In this model, we propose that γ-secretase activity, which controls the production of Aβ peptides, is also regulating the phosphorylation/inactivation of the protein phosphatase Slingshot1 (pSSH1). Reduced SSH1 phosphatase activity promotes an increase of Cofilin1 phosphorylation/inactivation (pCofilin1). Similarly, inactive pSSH1 is no longer able to promote the dephosphorylation/inactivation of the LIMK1 protein kinase (LIMK1), thus contributing both directly and indirectly to maintaining elevated inactive pCofilin1 levels. Finally, the decreased pCofilin1 levels observed in mice lacking APP suggests that APP could promote Cofilin1 phosphorylation/inactivation. Whether the decrease of pCofilin1 observed in APP_{KO} mice is directly linked to the loss of the γ-secretase-dependent cleavage of APP needs further investigation (?). Altogether, increased pCofilin1 could be responsible for (i) synapse morphology alteration; (ii) impaired AMPA receptors trafficking and AMPA receptors-mediated responses; and (iii) decreased NMDA receptors-induced long term depression (LTD), which all together negatively affect cognitive processes. Arrow: stimulation; Red arrow: pathways found altered in our study.

Appendix A. Supplementary data

Supplementary data to this article can be found online at http://dx.doi.org/10.1016/j.bbadis.2014.10.004.

References

[1] H.W. Querfurth, F.M. LaFerla, Alzheimer's disease, N. Engl. J. Med. 362 (2010) 329–344.
[2] A. Kern, C. Behl, The unsolved relationship of brain aging and late-onset Alzheimer disease, Biochim. Biophys. Acta 1790 (2009) 1124–1132.
[3] A.Y. Hsia, E. Masliah, L. McConlogue, G.Q. Yu, G. Tatsuno, K. Hu, D. Kholodenko, R.C. Malenka, R.A. Nicoll, L. Mucke, Plaque-independent disruption of neural circuits in Alzheimer's disease mouse models, Proc. Natl. Acad. Sci. U. S. A. 96 (1999) 3228–3233.
[4] K. Hsiao, P. Chapman, S. Nilsen, C. Eckman, Y. Harigaya, S. Younkin, F. Yang, G. Cole, Correlative memory deficits, Abeta elevation, and amyloid plaques in transgenic mice, Science 274 (1996) 99–102.
[5] L.F. Lue, Y.M. Kuo, A.E. Roher, L. Brachova, Y. Shen, L. Sue, T. Beach, J.H. Kurth, R.E. Rydel, J. Rogers, Soluble amyloid beta peptide concentration as a predictor of synaptic change in Alzheimer's disease, Am. J. Pathol. 155 (1999) 853–862.
[6] C.A. McLean, R.A. Cherny, F.W. Fraser, S.J. Fuller, M.J. Smith, K. Beyreuther, A.I. Bush, C.L. Masters, Soluble pool of Abeta amyloid as a determinant of severity of neurodegeneration in Alzheimer's disease, Ann. Neurol. 46 (1999) 860–866.
[7] R. Medeiros, M.A. Chabrier, F.M. LaFerla, Elucidating the triggers, progression, and effects of Alzheimer's disease, J. Alzheimers Dis. 33 (Suppl. 1) (2013) S195–S210.
[8] J. Hardy, The amyloid hypothesis for Alzheimer's disease: a critical reappraisal, J. Neurochem. 110 (2009) 1129–1134.
[9] D.J. Selkoe, Alzheimer's disease is a synaptic failure, Science 298 (2002) 789–791.
[10] S. Varadarajan, S. Yatin, M. Aksenova, D.A. Butterfield, Review: Alzheimer's amyloid beta-peptide-associated free radical oxidative stress and neurotoxicity, J. Struct. Biol. 130 (2000) 184–208.
[11] D.A. Butterfield, J. Drake, C. Pocernich, A. Castegna, Evidence of oxidative damage in Alzheimer's disease brain: central role for amyloid beta-peptide, Trends Mol. Med. 7 (2001) 548–554.
[12] D.A. Butterfield, The 2013 SFRBM discovery award: Selected discoveries from the butterfield laboratory of oxidative stress and its sequela in brain in cognitive disorders exemplified by Alzheimer disease and chemotherapy induced cognitive impairment, Free Radic. Biol. Med. 74C (2014) 157–174.
[13] W.L. Klein, Synaptotoxic amyloid-beta oligomers: a molecular basis for the cause, diagnosis, and treatment of Alzheimer's disease? J. Alzheimers Dis. 33 (Suppl. 1) (2013) S49–S65.
[14] C. Haass, A.Y. Hung, M.G. Schlossmacher, T. Oltersdorf, D.B. Teplow, D.J. Selkoe, Normal cellular processing of the beta-amyloid precursor protein results in the secretion of the amyloid beta peptide and related molecules, Ann. N. Y. Acad. Sci. 695 (1993) 109–116.
[15] C.A. Saura, S.Y. Choi, V. Beglopoulos, S. Malkani, D. Zhang, B.S. Shankaranarayana Rao, S. Chattarji, R.J. Kelleher 3rd, E.R. Kandel, K. Duff, A. Kirkwood, J. Shen, Loss of presenilin function causes impairments of memory and synaptic plasticity followed by age-dependent neurodegeneration, Neuron 42 (2004) 23–36.
[16] Y. Mitani, J. Yarimizu, K. Saita, H. Uchino, H. Akashiba, Y. Shitaka, K. Ni, N. Matsuoka, Differential effects between gamma-secretase inhibitors and modulators on cognitive function in amyloid precursor protein-transgenic and nontransgenic mice, J. Neurosci. Off. J. Soc. Neurosci. 32 (2012) 2037–2050.
[17] S.H. Nam, S.J. Seo, J.S. Goo, J.E. Kim, S.I. Choi, H.R. Lee, I.S. Hwang, S.W. Jee, S.H. Lee, C.J. Bae, J.Y. Park, H.S. Kim, S.B. Shim, D.Y. Hwang, Pen-2 overexpression induces Abeta-42 production, memory defect, motor activity enhancement and feeding behavior dysfunction in NSE/Pen-2 transgenic mice, Int. J. Mol. Med. 28 (2011) 961–971.
[18] B.P. Imbimbo, G.A. Giardina, gamma-secretase inhibitors and modulators for the treatment of Alzheimer's disease: disappointments and hopes, Curr. Top. Med. Chem. 11 (2011) 1555–1570.
[19] A. Haapasalo, D.M. Kovacs, The many substrates of presenilin/gamma-secretase, J. Alzheimers Dis. 25 (2011) 3–28.
[20] F.X. Guix, T. Wahle, K. Vennekens, A. Snellinx, L. Chavez-Gutierrez, G. Ill-Raga, E. Ramos-Fernandez, C. Guardia-Laguarta, A. Lleo, M. Arimon, O. Berezovska, F.J. Munoz, C.G. Dotti, B. De Strooper, Modification of gamma-secretase by nitrosative stress links neuronal ageing to sporadic Alzheimer's disease, EMBO Mol. Med. 4 (2012) 660–673.
[21] I. Benilova, E. Karran, B. De Strooper, The toxic Abeta oligomer and Alzheimer's disease: an emperor in need of clothes, Nat. Neurosci. 15 (2012) 349–357.
[22] D.M. Hartley, D.M. Walsh, C.P. Ye, T. Diehl, S. Vasquez, P.M. Vassilev, D.B. Teplow, D.J. Selkoe, Protofibrillar intermediates of amyloid beta-protein induce acute electrophysiological changes and progressive neurotoxicity in cortical neurons, J. Neurosci. Off. J. Soc. Neurosci. 19 (1999) 8876–8884.
[23] D.M. Walsh, I. Klyubin, J.V. Fadeeva, W.K. Cullen, R. Anwyl, M.S. Wolfe, M.J. Rowan, D.J. Selkoe, Naturally secreted oligomers of amyloid beta protein potently inhibit hippocampal long-term potentiation in vivo, Nature 416 (2002) 535–539.
[24] J.P. Cleary, D.M. Walsh, J.J. Hofmeister, G.M. Shankar, M.A. Kuskowski, D.J. Selkoe, K.H. Ashe, Natural oligomers of the amyloid-beta protein specifically disrupt cognitive function, Nat. Neurosci. 8 (2005) 79–84.
[25] K. Okamoto, T. Nagai, A. Miyawaki, Y. Hayashi, Rapid and persistent modulation of actin dynamics regulates postsynaptic reorganization underlying bidirectional plasticity, Nat. Neurosci. 7 (2004) 1104–1112.
[26] Y. Fukazawa, Y. Saitoh, F. Ozawa, Y. Ohta, K. Mizuno, K. Inokuchi, Hippocampal LTP is accompanied by enhanced F-actin content within the dendritic spine that is essential for late LTP maintenance in vivo, Neuron 38 (2003) 447–460.
[27] M.B. Rust, C.B. Gurniak, M. Renner, H. Vara, L. Morando, A. Gorlich, M. Sassoe-Pognetto, M.A. Banchaabouchi, M. Giustetto, A. Triller, D. Choquet, W. Witke, Learning, AMPA receptor mobility and synaptic plasticity depend on n-cofilin-mediated actin dynamics, EMBO J. 29 (2010) 1889–1902.

[28] J.J. Bravo-Cordero, M.A. Magalhaes, R.J. Eddy, L. Hodgson, J. Condeelis, Functions of cofilin in cell locomotion and invasion, Nat. Rev. Mol. Cell Biol. 14 (2013) 405–415.
[29] J. Gu, C.W. Lee, Y. Fan, D. Komlos, X. Tang, C. Sun, K. Yu, H.C. Hartzell, G. Chen, J.R. Bamburg, J.Q. Zheng, ADF/cofilin-mediated actin dynamics regulate AMPA receptor trafficking during synaptic plasticity, Nat. Neurosci. 13 (2010) 1208–1215.
[30] M. Van Troys, L. Huyck, S. Leyman, S. Dhaese, J. Vandekerkhove, C. Ampe, Ins and outs of ADF/cofilin activity and regulation, Eur. J. Cell Biol. 87 (2008) 649–667.
[31] G.C. Bellenchi, C.B. Gurniak, E. Perlas, S. Middei, M. Ammassari-Teule, W. Witke, N-cofilin is associated with neuronal migration disorders and cell cycle control in the cerebral cortex, Genes Dev. 21 (2007) 2347–2357.
[32] K. Mizuno, Signaling mechanisms and functional roles of cofilin phosphorylation and dephosphorylation, Cell. Signal. 25 (2013) 457–469.
[33] C.M. Hulette, K.A. Welsh-Bohmer, B. Crain, M.H. Szymanski, N.O. Sinclaire, A.D. Roses, Rapid brain autopsy. The Joseph and Kathleen Bryan Alzheimer's Disease Research Center experience, Arch. Pathol. Lab. Med. 121 (1997) 615–618.
[34] R. Radde, T. Bolmont, S.A. Kaeser, J. Coomaraswamy, D. Lindau, L. Stoltze, M.E. Calhoun, F. Jaggi, H. Wolburg, S. Gengler, C. Haass, B. Ghetti, C. Czech, C. Holscher, P.M. Mathews, M. Jucker, Abeta42-driven cerebral amyloidosis in transgenic mice reveals early and robust pathology, EMBO Rep. 7 (2006) 940–946.
[35] M.E. Calhoun, P. Burgermeister, A.L. Phinney, M. Stalder, M. Tolnay, K.H. Wiederhold, D. Abramowski, C. Sturchler-Pierrat, B. Sommer, M. Staufenbiel, M. Jucker, Neuronal overexpression of mutant amyloid precursor protein results in prominent deposition of cerebrovascular amyloid, Proc. Natl. Acad. Sci. U. S. A. 96 (1999) 14088–14093.
[36] M.G. Martin, S. Perga, L. Trovo, A. Rasola, P. Holm, T. Rantamaki, T. Harkany, E. Castren, F. Chiara, C.G. Dotti, Cholesterol loss enhances TrkB signaling in hippocampal neurons aging in vitro, Mol. Biol. Cell 19 (2008) 2101–2112.
[37] A.O. Sodero, L. Trovo, F. Iannilli, P. Van Veldhoven, C.G. Dotti, M.G. Martin, Regulation of tyrosine kinase B activity by the Cyp46/cholesterol loss pathway in mature hippocampal neurons: relevance for neuronal survival under stress and in aging, J. Neurochem. 116 (2011) 747–755.
[38] A.O. Sodero, C. Weissmann, M.D. Ledesma, C.G. Dotti, Cellular stress from excitatory neurotransmission contributes to cholesterol loss in hippocampal neurons aging in vitro, Neurobiol. Aging 32 (2011) 1043–1053.
[39] M. Pikkarainen, T. Kauppinen, I. Alafuzoff, Hyperphosphorylated tau in the occipital cortex in aged nondemented subjects, J. Neuropathol. Exp. Neurol. 68 (2009) 653–660.
[40] K. Tomobe, Y. Nomura, Neurochemistry, neuropathology, and heredity in SAMP8: a mouse model of senescence, Neurochem. Res. 34 (2009) 660–669.
[41] M.V. Aksenova, M.Y. Aksenov, W.R. Markesbery, D.A. Butterfield, Aging in a dish: age-dependent changes of neuronal survival, protein oxidation, and creatine kinase BB expression in long-term hippocampal cell culture, J. Neurosci. Res. 58 (1999) 308–317.
[42] N.M. Porter, O. Thibault, V. Thibault, K.C. Chen, P.W. Landfield, Calcium channel density and hippocampal cell death with age in long-term culture, J. Neurosci. Off. J. Soc. Neurosci. 17 (1997) 5629–5639.
[43] C. Lesuisse, L.J. Martin, Long-term culture of mouse cortical neurons as a model for neuronal development, aging, and death, J. Neurobiol. 51 (2002) 9–23.
[44] A. Herreman, D. Hartmann, W. Annaert, P. Saftig, K. Craessaerts, L. Serneels, L. Umans, V. Schrijvers, F. Checler, H. Vanderstichele, V. Baekelandt, R. Dressel, P. Cupers, D. Huylebroeck, A. Zwijsen, F. Van Leuven, B. De Strooper, Presenilin 2 deficiency causes a mild pulmonary phenotype and no changes in amyloid precursor protein processing but enhances the embryonic lethal phenotype of presenilin 1 deficiency, Proc. Natl. Acad. Sci. U. S. A. 96 (1999) 11872–11877.
[45] A. Herreman, G. Van Gassen, M. Bentahir, O. Nyabi, K. Craessaerts, U. Mueller, W. Annaert, B. De Strooper, gamma-Secretase activity requires the presenilin-dependent trafficking of nicastrin through the Golgi apparatus but not its complex glycosylation, J. Cell Sci. 116 (2003) 1127–1136.
[46] M. Cacquevel, L. Aeschbach, J. Houacine, P.C. Fraering, Alzheimer's disease-linked mutations in presenilin-1 result in a drastic loss of activity in purified gamma-secretase complexes, PLoS One 7 (2012) e35133.
[47] L. Zhao, Q.L. Ma, F. Calon, M.E. Harris-White, F. Yang, G.P. Lim, T. Morihara, O.J. Ubeda, S. Ambegaokar, J.E. Hansen, R.H. Weisbart, B. Teter, S.A. Frautschy, G.M. Cole, Role of p21-activated kinase pathway defects in the cognitive deficits of Alzheimer disease, Nat. Neurosci. 9 (2006) 234–242.
[48] L.S. Minamide, A.M. Striegl, J.A. Boyle, P.J. Meberg, J.R. Bamburg, Neurodegenerative stimuli induce persistent ADF/cofilin-actin rods that disrupt distal neurite function, Nat. Cell Biol. 2 (2000) 628–636.
[49] A.R. Gwon, J.S. Park, T.V. Arumugam, Y.K. Kwon, S.L. Chan, S.H. Kim, S.H. Baik, S. Yang, Y.K. Yun, Y. Choi, S. Kim, S.C. Tang, D.H. Hyun, A. Cheng, C.E. Dann 3rd, M. Bernier, J. Lee, W.R. Markesbery, M.P. Mattson, D.G. Jo, Oxidative lipid modification of nicastrin enhances amyloidogenic gamma-secretase activity in Alzheimer's disease, Aging Cell 11 (2012) 559–568.
[50] M.S. Kayser, M.J. Nolt, M.B. Dalva, EphB receptors couple dendritic filopodia motility to synapse formation, Neuron 59 (2008) 56–69.
[51] W.T. Kimberly, J.B. Zheng, T. Town, R.A. Flavell, D.J. Selkoe, Physiological regulation of the beta-amyloid precursor protein signaling domain by c-Jun N-terminal kinase JNK3 during neuronal differentiation, J. Neurosci. Off. J. Soc. Neurosci. 25 (2005) 5533–5543.
[52] M.J. Kim, S.J. Oh, S.H. Park, H.J. Kang, M.H. Won, T.C. Kang, J.B. Park, J.I. Kim, J. Kim, J.Y. Lee, Neuronal loss in primary long-term cortical culture involves neurodegeneration-like cell death via calpain and p35 processing, but not developmental apoptosis or aging, Exp. Mol. Med. 39 (2007) 14–26.
[53] M.T. Maloney, L.S. Minamide, A.W. Kinley, J.A. Boyle, J.R. Bamburg, Beta-secretase-cleaved amyloid precursor protein accumulates at actin inclusions induced in neurons by stress or amyloid beta: a feedforward mechanism for Alzheimer's disease, J. Neurosci. Off. J. Soc. Neurosci. 25 (2005) 11313–11321.
[54] A. Mendoza-Naranjo, E. Contreras-Vallejos, D.R. Henriquez, C. Otth, J.R. Bamburg, R.B. Maccioni, C. Gonzalez-Billault, Fibrillar amyloid-beta1-42 modifies actin organization affecting the cofilin phosphorylation state: a role for Rac1/cdc42 effector proteins and the slingshot phosphatase, J. Alzheimers Dis. 29 (2012) 63–77.
[55] J.A. Woo, A.R. Jung, M.K. Lakshmana, A. Bedrossian, Y. Lim, J.H. Bu, S.A. Park, E.H. Koo, I. Mook-Jung, D.E. Kang, Pivotal role of the RanBP9-cofilin pathway in Abeta-induced apoptosis and neurodegeneration, Cell Death Differ. 19 (2012) 1413–1423.
[56] T. Kim, G.S. Vidal, M. Djurisic, C.M. William, M.E. Birnbaum, K.C. Garcia, B.T. Hyman, C.J. Shatz, Human LilrB2 is a beta-amyloid receptor and its murine homolog PirB regulates synaptic plasticity in an Alzheimer's model, Science 341 (2013) 1399–1404.
[57] L. Heredia, P. Helguera, S. de Olmos, G. Kedikian, F. Sola Vigo, F. LaFerla, M. Staufenbiel, J. de Olmos, J. Busciglio, A. Caceres, A. Lorenzo, Phosphorylation of actin-depolymerizing factor/cofilin by LIM-kinase mediates amyloid beta-induced degeneration: a potential mechanism of neuronal dystrophy in Alzheimer's disease, J. Neurosci. Off. J. Soc. Neurosci. 26 (2006) 6533–6542.
[58] W. Morishita, H. Marie, R.C. Malenka, Distinct triggering and expression mechanisms underlie LTD of AMPA and NMDA synaptic responses, Nat. Neurosci. 8 (2005) 1043–1050.
[59] Y. Wang, Q. Dong, X.F. Xu, X. Feng, J. Xin, D.D. Wang, H. Yu, T. Tian, Z.Y. Chen, Phosphorylation of cofilin regulates extinction of conditioned aversive memory via AMPAR trafficking, J. Neurosci. Off. J. Soc. Neurosci. 33 (2013) 6423–6433.
[60] E.Y. Yuen, W. Liu, T. Kafri, H. van Praag, Z. Yan, Regulation of AMPA receptor channels and synaptic plasticity by cofilin phosphatase Slingshot in cortical neurons, J. Physiol. 588 (2010) 2361–2371.
[61] Q.L. Ma, F. Yang, F. Calon, O.J. Ubeda, J.E. Hansen, R.H. Weisbart, W. Beech, S.A. Frautschy, G.M. Cole, p21-activated kinase-aberrant activation and translocation in Alzheimer disease pathogenesis, J. Biol. Chem. 283 (2008) 14132–14143.
[62] B.W. Bernstein, J.R. Bamburg, ADF/cofilin: a functional node in cell biology, Trends Cell Biol. 20 (2010) 187–195.
[63] Y. Shi, C.G. Pontrello, K.A. DeFea, L.F. Reichardt, I.M. Ethell, Focal adhesion kinase acts downstream of EphB receptors to maintain mature dendritic spines by regulating cofilin activity, J. Neurosci. Off. J. Soc. Neurosci. 29 (2009) 8129–8142.
[64] L.Y. Chen, C.S. Rex, M.S. Casale, C.M. Gall, G. Lynch, Changes in synaptic morphology accompany actin signaling during LTP, J. Neurosci. Off. J. Soc. Neurosci. 27 (2007) 5363–5372.
[65] A.C. Paula-Lima, J. Brito-Moreira, S.T. Ferreira, Deregulation of excitatory neurotransmission underlying synapse failure in Alzheimer's disease, J. Neurochem. 126 (2013) 191–202.
[66] N.W. Hu, T. Ondrejcak, M.J. Rowan, Glutamate receptors in preclinical research on Alzheimer's disease: update on recent advances, Pharmacol. Biochem. Behav. 100 (2012) 855–862.
[67] S. Camandola, M.P. Mattson, Aberrant subcellular neuronal calcium regulation in aging and Alzheimer's disease, Biochim. Biophys. Acta 1813 (2011) 965–973.
[68] M.T. Maloney, J.R. Bamburg, Cofilin-mediated neurodegeneration in Alzheimer's disease and other amyloidopathies, Mol. Neurobiol. 35 (2007) 21–44.
[69] Q.L. Ma, F. Yang, S.A. Frautschy, G.M. Cole, PAK in Alzheimer disease, Huntington disease and X-linked mental retardation, Cell. Logist. 2 (2012) 117–125.
[70] S. Bellani, A. Mescola, G. Ronzitti, H. Tsushima, S. Tilve, C. Canale, F. Valtorta, E. Chieregatti, GRP78 clustering at the cell surface of neurons transduces the action of exogenous alpha-synuclein, Cell Death Differ. (2014), http://dx.doi.org/10.1038/cdd.2014.111 (in press).
[71] M. Bentahir, O. Nyabi, J. Verhamme, A. Tolia, K. Horre, J. Wiltfang, H. Esselmann, B. De Strooper, Presenilin clinical mutations can affect gamma-secretase activity by different mechanisms, J. Neurochem. 96 (2006) 732–742.
[72] M. Citron, D. Westaway, W. Xia, G. Carlson, T. Diehl, G. Levesque, K. Johnson-Wood, M. Lee, P. Seubert, A. Davis, D. Kholodenko, R. Motter, R. Sherrington, B. Perry, H. Yao, R. Strome, I. Lieberburg, J. Rommens, S. Kim, D. Schenk, P. Fraser, P. St George Hyslop, D.J. Selkoe, Mutant presenilins of Alzheimer's disease increase production of 42-residue amyloid beta-protein in both transfected cells and transgenic mice, Nat. Med. 3 (1997) 67–72.
[73] K. Duff, C. Eckman, C. Zehr, X. Yu, C.M. Prada, J. Perez-tur, M. Hutton, L. Buee, Y. Harigaya, D. Yager, D. Morgan, M.N. Gordon, L. Holcomb, L. Refolo, B. Zenk, J. Hardy, S. Younkin, Increased amyloid-beta42(43) in brains of mice expressing mutant presenilin 1, Nature 383 (1996) 710–713.